



**Bending creep behaviour of various polymer films analysed
by surface strain measurement**

Journal:	<i>Soft Matter</i>
Manuscript ID	SM-ART-11-2023-001566.R2
Article Type:	Paper
Date Submitted by the Author:	24-Feb-2024
Complete List of Authors:	Yu, Jiayi; Tokyo Institute of Technology Institute of Innovative Research, Laboratory for Chemistry and Life Science Kishino, Masayuki; Tokyo Institute of Technology Institute of Innovative Research, Laboratory for Chemistry and Life Science Hisano, Kyohei; Tokyo Institute of Technology Institute of Innovative Research, Laboratory for Chemistry and Life Science Shishido, Atsushi; Tokyo Institute of Technology Institute of Innovative Research, Laboratory for Chemistry and Life Science

PAPER

Bending creep behaviour of various polymer films analysed by surface strain measurement

Jiayi Yu^{ab}, Masayuki Kishino^{ab}, Kyohei Hisano^{ab}, and Atsushi Shishido^{*abc}

Received 00th January 20xx,
Accepted 00th January 20xx

DOI: 10.1039/x0xx00000x

Understanding the temporal bending deformation of polymer films is key to designing mechanically durable flexible electronic devices. However, such creep behaviour under persistent bending remains unclear due to a lack of precise and accurate bending strain analysis methods. Herein, we quantitatively analysed the bending creep behaviour of various polymeric films using our developed strain measurement method that can precisely measure surface strain from optical diffraction. The surface strain measurement reveals that bending creep deformation differs depending on the polymer structure. The four-element Burgers model was employed to model the temporal strain increase on the bending surface successfully. By fitting the four-element model to the time course of the measured surface strain, we found that each polymer film has a different threshold surface strain for the appearance of bending creep deformation. Such disparity in the bending creep behaviour can be explained by the difference in strain energy density between the polymer films and their elastic model; polymer films with small strain energy density difference show small bending creep deformation. The results obtained in this study contribute to the elucidation of the bending creep behaviour of polymer films and the development of flexible electronic devices operated under persistent bending.

1. Introduction

Polymer films are widely used in various fields due to their excellent properties, such as flexibility and processability. One of their promising applications is the substrate of flexible devices including displays, sensors, solar cells, and wearable electronics.^{1–6} The long-term reliability and durability of flexible devices heavily rely on the resistance of the polymer films to increased surface strains. Studies showed that the inorganic materials fabricated on a polymer substrate, such as electrodes and semiconductors, often fracture at small strains (<2%), leading to electrical failure and functional degradation.^{7–9} Therefore, understanding and improving the deformation resistance of polymer films is crucial for the development of reliable and long-lasting flexible devices.

Polymers undergo irreversible deformation over time, known as creep, when subjected to continuous mechanical stress. The creep deformation occurs due to their viscosity, which measures their resistance to flow.¹⁰ Creep deformation in polymer substrates causes a rise in surface strain, leading to the gradual degradation of flexible device performance. Essentially,

when flexible devices are maintained in a specific bending position without applying additional force, the surface undergoes continuous deformation due to constant external strain, ultimately resulting in performance degradation. Extensive studies have been conducted over the past few decades to comprehend the creep behaviour of polymers.^{10–13} These studies, focusing on tensile deformation, investigated the deformation mechanism of creep through computational and predicted the creep behaviour using theoretical approaches. However, research on the bending creep behaviour of thin polymer films has been limited, leaving a significant gap in our understanding of the bending creep behaviour of polymer films. Bending creep is a complex phenomenon that presents a significant challenge due to the following two points: the intricate spatial stress/strain distribution under bending and the requirement of a comprehensive understanding of the microscopic strain changes occurring at the nanometer scale. However, there is a significant lack of research on the bending creep of polymer films. Existing studies primarily focus on analytical models and simulations for polymeric beams,^{14–16} but few experimental studies have been done. Experimental studies targeting bending creep in polymer films are notably scarce. This limitation can be attributed to the challenges associated with accurately and precisely measuring strain in bent polymer films using conventional methods such as curvature analysis,^{17–19} strain gauges,^{20–23} and the digital image correlation (DIC) method.^{24–27} Although these methods have the capability to measure surface strain in bending polymer films, their effectiveness is limited by various experimental constraints: e.g., curvature analysis suffers from the interference of light

^a Laboratory for Chemistry and Life Science, Institute of Innovative Research, Tokyo Institute of Technology, Yokohama 226-8501, Japan

^b Department of Chemical Science and Engineering, School of Materials and Chemical Technology, Tokyo Institute of Technology, Meguro, Tokyo 152-8552, Japan

^c Living Systems Materialogy (LISM) Research Group, International Research Frontiers Initiative (IRFI), Tokyo Institute of Technology, Yokohama 226-8501, Japan

E-mail: ashishid@res.titech.ac.jp

caused by bending, which affects accurate measurements and reduces the reliability of results. Strain gauges, the most common method for measuring bending strain, introduce external connections to electrodes, disturbing the bending behaviour of the polymer films. While the DIC method has gained attention for its ability to quantify strain on the cross-section of polymer films, challenges arise in creating speckle patterns necessary for accurate measurements. To gain deeper insights into the phenomenon of bending creep, developing a precise and accurate strain analysis method is imperative.

To overcome the issue, we previously developed the surface-labeled grating method utilizing optical diffraction to quantify surface strain in bending polymer films.^{28–30} In this method, a soft thin-film grating label is attached to a polymer film to directly measure the surface strain in real-time without affecting the material's bending behaviour. Utilizing a laser beam with a diameter of mere 100–200 μm , we achieved highly localized strain measurements. Earlier studies demonstrated the method's remarkable capability to quantify displacement at the nanometer scale (0.5–1.0 nm) with minimal error ($< \pm 0.05\%$ strain).²⁹ This unmatched precision distinguishes the surface-labeled grating method as a robust tool for quantitatively measuring surface bending strain in flexible films. This powerful method enables the detection of a slight strain change on the surface of polymer films, allowing for a deeper understanding of the bending creep behaviour of polymer films.

In this study, we employed the surface-label grating method to reveal the creep behaviour of various polymer films under persistent bending. Our focus is on practical scenarios where materials undergo continuous external strain. It is crucial to note that, rather than pure creep (as defined by strain change under constant force), this study delves into a combined phenomenon of creep and stress relaxation—technically, the temporal surface strain changes under constant external pressed distance at both film ends. For simplicity, we use the term "creep" throughout the discussion. Additionally, we employ the four-element model to fit experimental data, offering a relatively straightforward yet effective framework for assessing the temporal change in surface strain. This model serves as a valuable tool for quantitatively exploring the complex bending creep phenomena. The surface strain measurement revealed that the bending creep behaviour varied depending on the polymer structure. The explanation of polymer structure-dependent creep behaviour was achieved through the strain energy density difference between the polymer films and their elastic model. Furthermore, we observed that polymers with non-linear elasticity at small strains exhibited bending creep at small surface strains, while polymers with higher viscosity experienced greater creep deformation. These findings suggest that the viscoelastic behaviour obtained from tensile tests can be used to predict the bending creep behaviour of polymer films, providing valuable insights for the efficient design of flexible electronic device substrates. Future research focusing on micro/mesoscale analysis of molecular structures and higher-ordered structures, quantitative analysis of inner surface creep behaviour, and investigation of the effects of temperature and bending strain

rate on polymer films would open a pathway for developing highly durable, flexible applications in the field of soft robotics and flexible electronics.

2. Experimental

2.1 Materials

The following polymer films, which are used for substrates of flexible electronic devices, were selected for the analysis in this study: polyethylene terephthalate (PET; Lumirror T60, Toray Industries Inc., Japan), polyethylene naphthalate (PEN; Teonex Q51, Toyobo Co., Ltd., Japan), polyvinyl chloride (PVC; Sankyo Kagaku Yakuhin Co., Ltd., Japan), and polycarbonate (PC; Lupilon FE-2000, Mitsubishi Gas Chemical Company, Inc., Japan). The polymer main chain orientation of these films was identified using a polarized optical microscope (POM, BX50, Olympus Corp., Japan) as shown in Fig. S1 (ESI[†]). The main chain orientation of PVC and PC films was determined by the additive and subtractive colours using a tint plate, while that of PEN and PET films could not be identified due to their high retardation. Their optical axes were further investigated by attenuated total reflectance infrared spectroscopy (ATR-IR; FTIR-6600, JASCO Co.) equipped with polarizers. As shown in Fig. S2 (ESI[†]), the polarized IR spectra exhibited dichroism depending on the optical axes. The main chain orientations of the PEN and PET films were identified from the absorption near 1087 cm^{-1} due to C–O–C stretching vibration whose direction is generally parallel to the orientation.³¹

For bending strain measurements, all films were cut into dimensions of 40 mm in length and 30 mm in width. The identified main chain orientation and the film long axis are parallel. For tensile tests, all films were cut into dumbbell shapes with a gauge length and centre part width of 25 and 4 mm, respectively, using a dumbbell cutter (SDMK-1000, Dumbbell Co. Ltd., Japan).

2.2 Formation of thin grating label on polymer surface

Thin grating labels were formed on the surface of the targeted polymer films (Fig. S3, ESI[†]). Polydimethylsiloxane (PDMS) was selected as the label because of its softness (Young's modulus ~ 2 MPa).⁹ A PDMS precursor solution was prepared using a base compound and curing agent in a weight ratio of 10:1 (SILPOT 184 W/C, Dow Corning Toray Co. Ltd., Japan). The solution was stirred at 25 $^{\circ}\text{C}$ for 15 min and then degassed under reduced pressure. The solution was dropped onto the targeted films. Note that prior to drop-casting of the solution, ozone treatment was conducted for 5 min using an ozone cleaner (SSPL17-110, SEN Lights Corp., Japan) for PC films to improve the adhesion of PDMS. Then, a polymeric mold with a grating structure of which period is 4.0 μm and depth is 450 nm (Kyodo International, Inc., Japan) was placed onto the solution. Then the solution was heated and cured to form a thin PDMS grating label on the film surface: the heating conditions depended on polymer structures considering their glass transition temperature: 12 h at 55 $^{\circ}\text{C}$ for PVC films, 6.5 h at 60 $^{\circ}\text{C}$ for PET films, and 3.5 h at 75 $^{\circ}\text{C}$ for PC and PEN films.

2.3 Surface strain measurement

The optical setup of surface strain measurement is shown in Fig. 1. A He–Ne laser beam with a wavelength (λ) of 633 nm was normally incident to the grating label on the polymer films, yielding diffraction. Bending films induces strain on the surface, which changes the grating period (Λ) of the label, diffraction angle (α), and the distance between the -1 st and $+1$ st diffracted beams (D) on the screen. Therefore, the surface bending strain (ϵ_s) can be evaluated as follows. First, D was detected using a CCD camera 2 (Fig. S4, ESI[†]). From D and the length between the screen and a film (l), $\alpha = \arctan(D/l)$ was obtained. It should be noted l was kept to 55.019 mm with an automatic stage controller during the measurement. The Λ was yielded from $\lambda/\sin\alpha$. The ϵ_s was calculated from the ratio of a change in the grating period ($\Delta\Lambda$) to the grating period before bending ($\Lambda_0 = 4 \mu\text{m}$).

Polymer films were bent by pushing both edges; bending degree was controlled by an applied strain ($\Delta L/L$), where L is the initial film length and ΔL is the pushing distance. The applied strain rate was $8.75\% \text{ min}^{-1}$. The bending creep behaviour was evaluated by measuring a temporal change in ϵ_s of polymer films bent by each applied strain for 30 min. All measurements were taken at least three times for each film. Surface strain values and error bars in the figures represent the means and standard deviations of the respective measurement results.

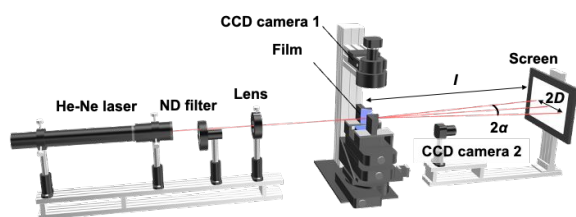


Fig. 1 Optical setup for the measurement of surface bending strains in a polymer film.

2.4 Tensile tests

A stress–strain (S – S) curve of each polymer film was measured by tensile tests performed using a tensile testing machine (Instron 5943, Instron Japan Co., Ltd., Japan). Each film was stretched up to 6% tensile strain with a strain rate of $0.35\% \text{ min}^{-1}$, which approximately corresponded to the increase rate of ϵ_s . The thicknesses of PET and PEN films for tensile tests were $188 \mu\text{m}$ and those of PVC and PC films were $200 \mu\text{m}$. Young's moduli were calculated from the range of 0.050 – 0.25% strain in S – S curves.

3. Results and discussion

3.1 Surface strain measurement of PVC films

The creep behaviour of polymer films was observed when they bent largely. Fig. 2a shows cross-sectional images of a flat and bent PVC film with a thickness of $200 \mu\text{m}$ as an example. Imposing 80% applied strain bent the PVC film largely. As displayed in the magnified view in Fig. 2a, holding the applied

strain at 80% for 30 min after the initial bending clearly sharpened the bending shape, indicating that the creep deformation occurred.

To quantify the temporal change in the bending shape, surface strain (ϵ_s) on the outer surface of the PVC films was measured using the surface-labeled grating method; then, we evaluated the temporal change of surface strain ($\Delta\epsilon_s$). Fig. 2b shows ϵ_s of the PVC films bent by 80, 70, 60, and 40% of applied strains. Bending the PVC films increased ϵ_s , showing that in-plane tension occurred on the outer bending surface. Subsequent measurement of ϵ_s under 30 min holding of the applied strain revealed that the increase in surface strain ($\Delta\epsilon_s$) differed depending on the holding applied strain: $\Delta\epsilon_s$ at 80, 70, 60, and 40% applied strains were 1.04, 0.17, 0.04, and 0.01%, respectively (Fig. 2c). In addition to the PVC films with a $200 \mu\text{m}$ thickness, surface strain of PVC films with 310 and $410 \mu\text{m}$ thicknesses for 30 min was measured (Fig. S5b–c, ESI[†]). The values of $\Delta\epsilon_s$ increased with the increase in the film thickness (Fig. 2d). The surface strain measurement using the developed method clarified that the bending creep deformation became larger as the applied strain and thickness increased. This observed behaviour was also noted in other bending polymer films as shown in Fig. S5 (ESI[†]). This phenomenon can be explained by the strain equation $\epsilon = z/R$, where R represents the radius of curvature, and z signifies the distance from the position of the neutral mechanical plane. Consequently, a larger applied strain corresponds to a smaller R , resulting in a larger strain (ϵ). Conversely, as z is positively related to thickness, a thicker film leads to a larger z , resulting in a larger ϵ . This relationship leads to a noticeable increase in surface strain in polymer films with large thicknesses under large applied strain. Notably, this increase in surface strain contributes to a subsequent increase in creep. This phenomenon will be further elucidated in section 3.3.

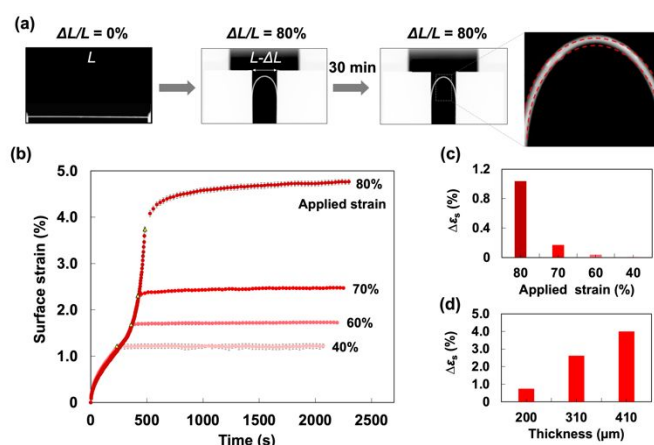


Fig. 2 (a) Cross-sectional images of a flat and bent PVC film with a $200 \mu\text{m}$ thickness. Inset shows a magnified image of the film bent for 30 min. The dashed red line represents the bent shape at the beginning of the holding process. (b) Surface strain of PVC films with a $200 \mu\text{m}$ thickness bent by 80, 70, 60, and 40% applied strains. Yellow triangles signify the start of the constant holding state. (c) Increase in surface strain ($\Delta\epsilon_s$) of the PVC films with a $200 \mu\text{m}$ thickness bent by each applied strain for 30 min. (d) Increase in surface strain of the PVC films with 200, 310, and $410 \mu\text{m}$ thicknesses bent by 70% applied strain for 30 min.

Furthermore, we can see that different polymer materials exhibit different degrees of bending strain and temporal strain changes, highlighting the role of polymer structures in influencing surface strain and fracture modes of bending polymer films, consistent with previous studies in our group.^{32, 33}

3.2 Four-element model fitting

For further analysis of the bending creep, a theoretical model was applied to the measured temporal changes of surface strain, $\Delta\varepsilon_s$. When polymers undergo deformation, their viscoelastic properties determine their response to applied stress and strain.⁸ Studies have demonstrated the significant role of viscoelasticity in the deformation mechanisms of polymers.^{34, 35} To better understand the behaviour of polymer materials, we utilized the four-element model, a theoretical creep model designed to describe the combined behaviour of viscosity and elasticity in materials. This model, also known as the Burgers model, has been used to describe the creep deformation of various viscoelastic materials.^{10, 15, 36, 37}

The four-element model consists of parallel and serial connections of a spring and a dashpot, where the spring symbolises the elastic element, and the dashpot the viscous element as illustrated in Fig. 3a, and is expressed as follows:

$$\varepsilon(t) = \varepsilon_0 + a [1 - \exp(-bt)] + ct \quad (1)$$

where ε is strain; t is the measurement time; $\varepsilon_0 (= \sigma/E_E)$ is the initial strain; a is σ/E_V ; b is E_V/η_{V1} ; c is σ/η_{VP} ; σ is the applied stress; E_E and η_P are modulus and viscosity of the Maxwell spring and dashpot, respectively; E_V and η_V are modulus and viscosity of the Kelvin-Voigt spring and dashpot, respectively. The first term represents the instantaneous strain (ε_0); the second term describes the delayed elasticity of the Kelvin-Voigt unit and dominant in the earliest stage of creep; the third term is the viscous flow, which appears after a sufficiently long time period of loading.

The bending creep behaviour of the polymer films was evaluated using the four-element model. Prior to model fitting, the surface strain of the polymer films was replotted with the start time of the holding state as 0 s. Using 200 μm -thick PVC film as an example, the 30 min-long creep data measured after bent to an applied strain of 80% was expressed using the four-element model (Fig. 3b). Notably, the model exhibited a robust fit, as evident from the minimal and evenly distributed residual plot (Fig. 3b, top), indicating its qualitative representation of the observed phenomenon. Therefore, the four-element model (Eq. 1), can be used to represent the relationship between surface strain and measurement time. The fitting model at 0 s is designated as the initial surface strain (ε_0). Three coefficients are iteratively optimized to minimize the sum of squared differences, serving to quantify the disparity between predicted values from the model and actual experimental data. This optimization process allows for the determination of coefficients that best fit the experimental data. Coefficient 'a' signifies the magnitude of strain increase in the early stage of creep, the start of the holding bending state; coefficient 'b'

means the reciprocal of the retardation time of the model, which can not be readily visually represented in the graph; coefficient 'c' represents the creep rate of the later steady creep stage. It is essential to note that the original configuration of the four-element model assumed a constant force, which is different from the conditions in this study. Therefore, the parameters do not directly indicate viscoelasticity but rather evaluate the temporal strain increase phenomenon due to viscoelasticity. 'a' is defined as strain increase factor, as it reflects the degree of temporal surface strain increase soon afterward the polymer film is bent to a specific applied strain and maintained in a stationary state (Fig. 3b, top). This model fitting process effectively characterizes and quantifies the observed behaviour, providing valuable insights to the bending creep deformation in a 30-min time span.

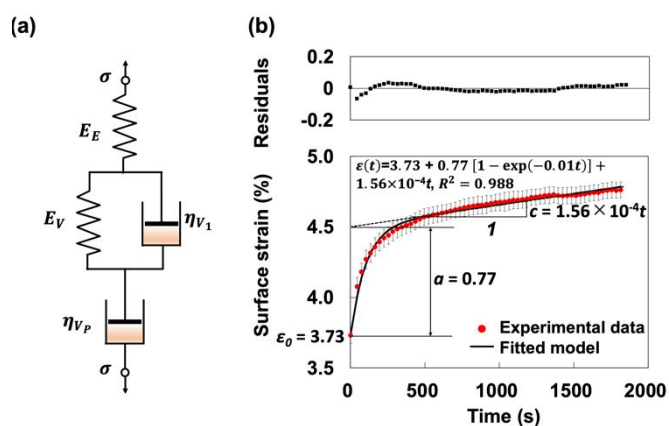


Fig. 3 (a) Schematic illustration of four-element model. σ is the applied stress, E_E , E_V are the elastic modulus of both springs and η_V , η_P are the viscosities of both dashpots. (b) Modelling the surface strain increase using the four-element model based on measured data: PVC, 200 μm , 80% applied strain. Coefficient 'a' signifies the magnitude of large strain increase in the early stage of creep, at the start of the holding bending state; c signifies the slope of strain increase data in the later steady-state stage. The top of (b) displays the residual plot.

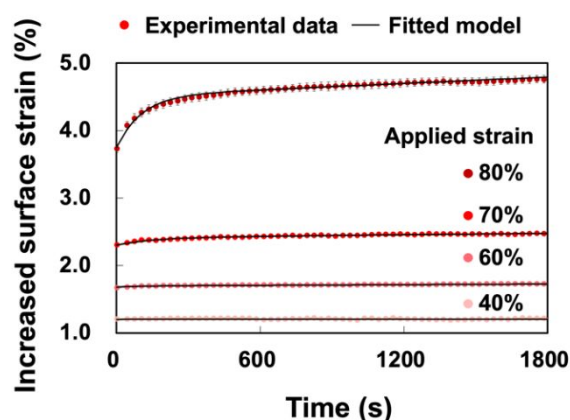


Fig. 4 Experimentally measured (dots) and theoretically fitted (line) surface strains over 30 minutes for 200 μm -thick PVC films under various constant applied strains.

Fig. 4 shows the curve fitting for the 30-minute creep tests on 200 μm -thick PVC films under different applied strains. Table 1 summarizes the modeling results. The model coefficients, namely a , b , and c , exhibit variations corresponding to the applied strains. Additionally, the temporal change of surface strains of the PVC films with 310 and 410 μm thicknesses were also analysed by the four-element model.

Table 1 Average values of parameters obtained from the curve fitting of the Burgers model on 200 μm -thick PVC films under various applied strains ε_a .

ε_a (%)	ε_0 (%)	a	b	c
80	3.73	0.770	0.010	1.56×10^{-4}
70	2.30	0.111	0.006	3.49×10^{-5}
60	1.68	0.017	0.029	1.66×10^{-5}
40	1.21	0.003	0.024	0

3.3 Bending creep behaviour depending on the surface strain

To comprehensively understand the bending creep behaviour of various polymer films, the relation between a , the strain increase factor, and the initial surface strain (ε_0) of each polymer film with different thicknesses was investigated. The investigation was conducted through the surface strain measurement and four-element model fitting as shown in Fig. 5a–d. The result revealed that for all materials, the value of a begins to increase above a certain ε_0 regardless of film thickness, indicating the existence of a threshold surface strain (ε_t) for the onset of the bending creep.

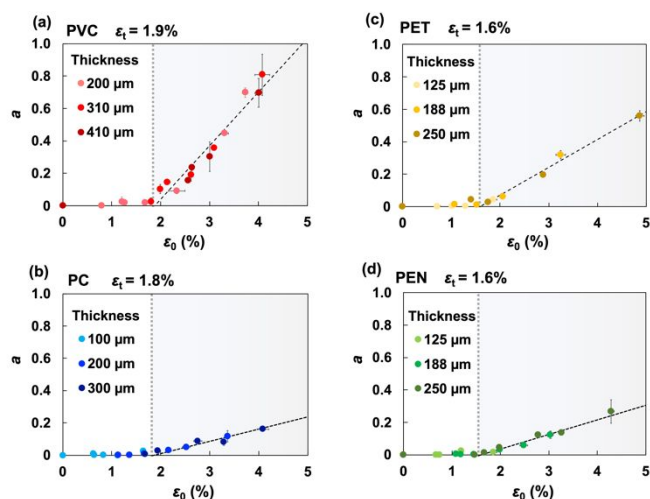


Fig. 5 Strain increase factor a as a function of threshold strain ε_t : (a) PVC, (b) PC, (c) PET, and (d) PEN.

Examining the original function Eq. 1, formulated for tensile creep where ε_0 is σ/E_E , and a is σ/E_V , these two parameters were expected to exhibit linear proportionality. However, the observed result showed a delay for the onset of the bending creep. Despite recognizing the non-constant force on the surface of the polymer films, a suitable fit and coefficients can

be determined. Thus, it is reasonable to assume that the variable σ in the function remains consistent across all terms containing σ . While ε_0 and a should have shown a linear relationship, a delay in the linear relation is observed, with ' a ' starting to increase only beyond a certain threshold value.

This intriguing result may be attributed to the unique bending behaviour, where the compressive force on the inner surface interferes with the deformation on the stretched outer surface. The inner surface strain on PET films is measured utilizing the surface-labeled grating method with the same experimental procedure, as illustrated in Fig. S6, ESI[†]. Notably, the inner surface exhibits a similar trend to the outer surface, but with a slightly larger ε_0 . Consequently, the creep increase factor, ' a ', is also marginally larger (Table S1). Consistent with previous studies by Taguchi *et al.*,²⁹ an asymmetrical behaviour between the inner and outer surfaces is observed in PEN films, with the strain on the inner surface surpassing that of the outer surface. These findings suggest that, in contrast to pure uniaxial tensile behavior, the inner and outer surfaces of bending polymer films exhibit differences, potentially resulting in a distinctive bending creep behavior. Subsequent investigations will delve deeper into this aspect, taking into account influences from the spatial movement of molecular chains within the film. However, our current study focuses on examining the occurrence of the bending creep phenomenon, including the threshold values, which may be due to the structural and mechanical property differences in polymer films. This investigation is essential for providing guidelines to reduce temporal bending deformation in flexible devices.

To evaluate the threshold surface strain, a linear fit was applied to the plot where ' a ' is not negligible (above 0.03%). The line that provided the best fit to the data was employed. The point of intersection between the line and the x-axis determines the threshold surface strain values (ε_t). The values of ε_t were found to be approximately 1.9%, 1.8%, 1.6%, and 1.6% for PVC, PC, PET, and PEN films, respectively. Furthermore, the degree of the increase in a differs among the polymer films, with the values of a being larger in the order of PVC>PET>PEN>PC at ε_0 above 4%. These findings show that the occurrence of the bending creep was determined by the surface strain, and the bending creep behaviour depends on polymer structures.

3.4 Discussion on bending creep behaviour

To elucidate the bending creep behaviour of the PVC, PC, PET, and PEN films, their stress–strain (S–S) relation was examined by tensile tests. As shown in Fig. 6a, the polymer films showed different S–S curves: PET and PEN films required larger stress than PVC and PC films at the same tensile strain. All materials initially display a linear elastic region, where the stress increases linearly with strain, following Hooke's law. At the higher strain region, the response becomes nonlinear.

To compare their nonlinearity, we employed elastic deformation region represented by the linear part of the S–S curves and normalized the S–S curves by Young's modulus. The normalized S–S curves in Fig. 6b show that the polymer films exhibit elastic deformation up to approximately 1.0% tensile strain and then non-elastic deformation.

The non-elastic/plastic deformation of the polymer films was quantified by calculating an area enclosed by the normalized

S–S curves and a line of Hooke's law. The area represents the strain energy density difference (SEDD) between the polymer films and elastic material. The SEDD is attributed to plastic deformation caused by the viscosity in polymers. As displayed in Fig. 7, the SEDD of the polymer films has a threshold tensile

The bending creep behaviour of the polymer films can be explained by the SEDD. There is a positive correlation between the threshold strains of the bending creep and SEDD (Fig. 8a). This correlation demonstrates that the PET and PEN films, which begin non-elastic deformation earlier than the PVC and PC films, undergo the bending creep deformation at the smaller strain.

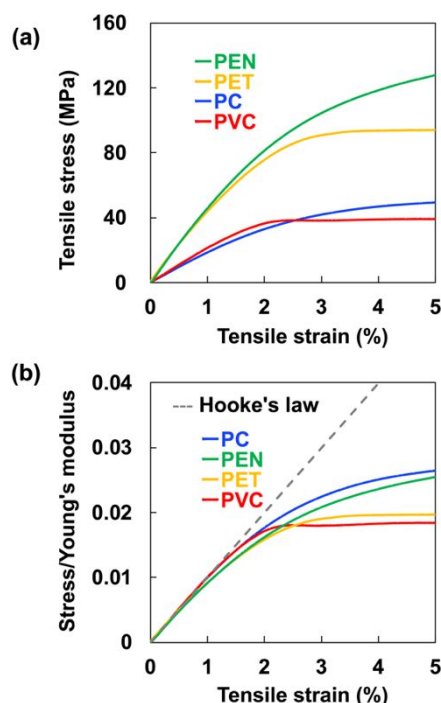


Fig. 6 (a) Stress-strain curves and (b) normalized stress-strain curves of PVC, PC, PEN, and PET films.

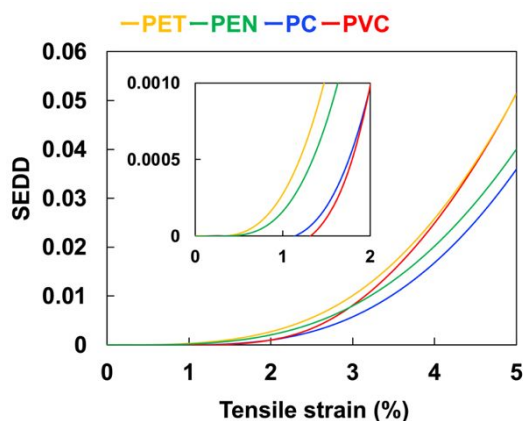


Fig. 7 SEDD of PVC, PC, PEN, and PET films as a function of tensile strain. The inset shows the magnification of tensile strain ranging from 0 to 2%.

strain and increases as the tensile strain increases. The threshold tensile strains for the SEDD of the PVC (1.32%) and PC films (1.15%) were larger than the PET (0.40%) and PEN films (0.38%), indicating that the PVC and PC films deform elastically up to the larger tensile strain. Furthermore, the SEDD of the PVC and PET films at plastic deformation strain regions surpasses that of the PC and PEN films. This shows that PVC and PET films deform more plastically under large strain conditions, signifying a more pronounced viscous behaviour.

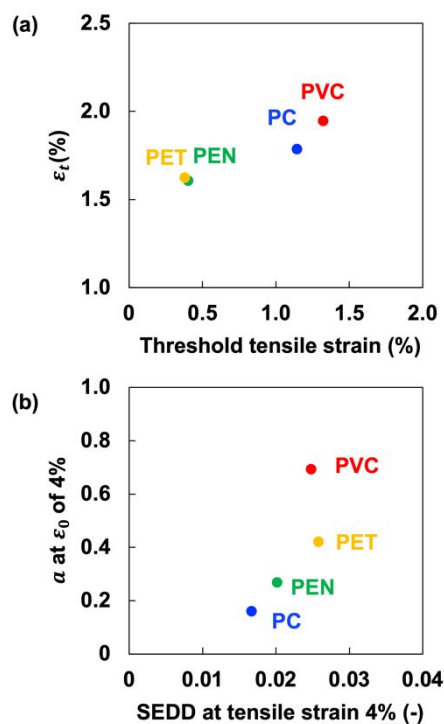


Fig. 8 (a) Correlation between the threshold strains of the bending creep and strain energy density difference (SEDD). (b) Correlation between the strain increase factor (α) at 4% initial surface strain and the SEDD at 4% tensile strain.

It is known that, for some semicrystalline polymers, irrecoverable deformation can arise from any applied stress.³⁸ The small SEDD of the semicrystalline polymers PEN and PET films is attributed to their composite structure and the presence of crystals. The crystalline region in these films disturb the neighboring amorphous regions, restricting their segmental mobility. This disturbance is evidenced by a wide distribution of glass transition temperatures in crystalline polymer materials.³⁹ Stress tends to concentrate in the undisturbed amorphous regions, which are far from rigid crystal regions. Consequently, this concentration of stress leads to irrecoverable plastic deformation of the polymer even under relatively small stress. Therefore, the small SEDD observed in the PEN and PET films can be explained by the combined effects of the composite structure and the behaviour of the undisturbed amorphous regions in these semicrystalline polymers.

In addition to the threshold strain, the magnitude of the bending creep was analyzed by plotting strain increase factor (α) at 4% surface strain as a function of the SEDD at 4% tensile strain (Fig. 8b). We found a positive correlation, showing that the PC and PEN films, which are relatively elastic materials, experience small creep deformation despite large bending. This trend persists across different levels of tensile strain during

plastic deformation, including 3, 4, and 5% (Fig. S7, ESI†). The resistance to creep deformation observed in the PC and PEN films may be derived from their more rigid molecular structures and stronger van der Waals force among polymer main chains compared to PVC and PET films.^{40,41} The presence of functional groups such as rigid aromatic rings, carbonyl group, and ester bonds in their polymer backbones, provides strong intermolecular force and thus strong mechanical strength and elastic properties to the films.⁴² In Fig. 8, it should be noted that the plot of the PVC film is distinct from the other plots of the PC, PEN, and PET films. This is attributed to crazes in the PVC films (Fig. S8, ESI†). These results indicate that the bending creep behaviour of polymer films can be predicted by the SEDD calculated from the normalized S–S curves.

4. Conclusions

In conclusion, the bending creep behaviour of the PVC, PC, PET, and PEN films was explored through the surface strain measurement, four-element model, and strain energy density. Our developed strain analysis method allowed us to precisely quantify the temporal change in the strain on the outer surface of the bent polymer films. In addition to the experimental analysis, the four-element model was fitted to the measured strain, and then the strain increase factor was evaluated. Interestingly, the strain increase factor (creep deformation) began to increase when the surface strain exceeded a critical value. Such bending creep behaviour can be accounted for by the strain energy density difference (SEDD) between the polymer films and elastic material: the SEDD represents an energy loss through deformation due to viscosity. The PET and PEN films whose threshold strain for the SEDD is small experienced the appearance of bending creep deformation under a small surface strain. On the other hand, the PC and PEN films showing a small SEDD underwent small bending creep deformation at large bending over 4% surface strain. These results indicate that we can predict the bending creep behaviour of the polymer films by analysing the SEDD, which is useful for efficiently designing polymer film substrates of flexible electronic devices.

The precise measurement of the surface bending strain, coupled with quantitative analysis using the four-element model provides valuable insights into the bending creep behaviour of various polymer film. This advancement holds promise for the development of mechanically durable flexible electronics and soft robots subjected to persistent bending. In our forthcoming research, we will conduct microscale analysis using X-ray and IR to deepen our understanding of the bending behaviour and elucidate the influence of molecular structures. Our plan also includes expanding the surface-labeled grating method to quantitatively measure compressive strain on the inner side of bending polymer films. Furthermore, we will explore the effects of temperature and bending rate on each surface, as well as delving into the processes of strain relaxation during bending to investigate viscoelasticity in polymer films. The present study serves as the cornerstone for our future research endeavours, with the overarching goal of unravelling

the complexities of creep and relaxation on both surfaces, clarifying their interplay, and contributing to a comprehensive understanding of bending behaviour in polymer films.

Author Contributions

AS conceived and planned the experiments; AS supervised the project; JY prepared the samples, performed the strain measurements, and analysed the experimental data with the support of MK, HK, and AS; MK helped with the measurement of optical properties; JY took the lead in writing the manuscript with the support of MK, KH, and AS. All authors have approved the final version of the manuscript.

Conflicts of interest

There are no conflicts to declare.

Acknowledgements

This work was supported by a Grant-in Aid for Scientific Research on Innovative Areas “Molecular Engine” (JSPS KAKENHI Grant Number JP18H05422). This work was supported by JSPS KAKENHI Grant Number JP22H02128 and by JST CREST Grant Number JPMJCR18I4, Japan. This work was performed under the cooperative research program of “Network Joint Research Center for Materials and Devices” and under the research program of “Dynamic Alliance for Open Innovation Bridging Human, Environment and Materials” at the Network Joint Research Center for Materials and Devices.

Notes and references

1. H. J. Kim, K. Sim, A. Thukral and C. Yu, *Sci. Adv.*, 2017, **3**, e1701114.
2. J. A. Rogers, T. Someya and Y. G. Huang, *Science*, 2010, **327**, 1603–1607.
3. M. Mizukami, S. I. Cho, K. Watanabe, M. Abiko, Y. Suzuri, S. Tokito and J. Kido, *IEEE Electr. Device L*, 2018, **39**, 39–42.
4. W. Seung, M. K. Gupta, K. Y. Lee, K. S. Shin, J. H. Lee, T. Y. Kim, S. Kim, J. Lin, J. H. Kim and S. W. Kim, *ACS Nano*, 2015, **9**, 3501–3509.
5. S. Park, S. W. Heo, W. Lee, D. Inoue, Z. Jiang, K. Yu, H. Jinno, D. Hashizume, M. Sekino, T. Yokota, K. Fukuda, K. Tajima and T. Someya, *Nature*, 2018, **561**, 516–521.
6. N. Akamatsu, K. Hisano, R. Tatsumi, M. Aizawa, C. J. Barrett and A. Shishido, *Soft Matter*, 2017, **13**, 7486–7491.
7. Z. Chen, B. Cotterell and W. Wang, *Eng. Fract. Mech.*, 2002, **69**, 597–603.
8. W. Kim, I. Lee, D. Y. Kim, Y. Y. Yu, H. Y. Jung, S. Kwon, W. S. Park and T. S. Kim, *Nanotechnol.*, 2017, **28**, 194002.
9. F. Nickel, T. Haas, E. Wegner, D. Bahro, S. Salehin, O. Kraft, P. A. Gruber and A. Colsmann, *Sol. Energ. Mat. Sol. C*, 2014, **130**, 317–321.
10. W. N. Findley, J. S. Lai and K. Onaran, *Creep and relaxation of nonlinear viscoelastic materials, with an introduction to*

- linear viscoelasticity*, North-Holland Pub. Co.: sole distributors for the U.S.A. and Canada, Elsevier/North Holland, Amsterdam; New York, 1976.
11. S. Jorik, A. Lion and M. Johlitz, *Polym. Test.*, 2019, **75**, 151–158.
 12. L. Ladouce, J. Perez, R. Vassoille and G. Vigier, *J. Mater. Sci.*, 1994, **29**, 5399–5406.
 13. L. H. Tam, R. D. Wu, M. A. N. Minkeng, J. Q. Jiang, A. Zhou, H. L. Hao, Z. C. Yu and C. Wu, *Mech. Adv. Mater. Struct.*, 2022, **30**, 4052–4064.
 14. B. B. Dai, R. L. Huo, K. Wang, Z. Q. Ma and H. Fang, *Polymers*, 2022, **14**, 4789.
 15. C. L. Dong, S. Zhang, J. Wang and Y. H. Chui, *Constr. Build. Mater.*, 2021, **269**, 121308.
 16. Y. Gao, F. Yu and P. Wu, *Thin Wall Struct.*, 2022, **174**, 109128.
 17. A. Jedaa and M. Halik, *Appl. Phys. Lett.*, 2009, **95**, 103309.
 18. K. Kuwahara, R. Taguchi, M. Kishino, N. Akamatsu, K. Tokumitsu and A. Shishido, *Appl. Phys. Express*, 2020, **13**, 056502.
 19. R. Taguchi, K. Kuwahara, N. Akamatsu and A. Shishido, *Soft Matter*, 2021, **17**, 4040–4046.
 20. Y. S. Rim, S. H. Bae, H. J. Chen, N. De Marco and Y. Yang, *Adv. Mater.*, 2016, **28**, 4415–4440.
 21. S. J. Lee, Y. Kim, J. Y. Hwang, J. H. Lee, S. Jung, H. Park, S. Cho, S. Nahm, W. S. Yang, H. Kim and S. H. Han, *Sci. Rep.*, 2017, **7**, 3131.
 22. Y. Yue, N. S. Liu, W. J. Liu, M. A. Li, Y. A. Ma, C. Luo, S. L. Wang, J. Y. Rao, X. K. Hu, J. Su, Z. Zhang, Q. Huang and Y. H. Gao, *Nano Ener.*, 2018, **50**, 79–87.
 23. H. Nesser and G. Lubineau, *ACS Appl. Mater. Interfaces*, 2021, **13**, 36062–36070.
 24. W. Jo, T. I. Lee and T. S. Kim, *Microelectron. Reliab.*, 2022, **130**, 114485.
 25. Y. Lee, H. Lee, H. G. Im, W. Jo, G. M. Choi, T. S. Kim, J. Jang and B. S. Bae, *Compos. B. Eng.*, 2022, **247**, 110336.
 26. T. I. Lee, W. Jo, W. Kim, J. H. Kim, K. W. Paik and T. S. Kim, *ACS Appl. Mater. Interfaces*, 2019, **11**, 13416–13422.
 27. W. Jo, H. Lee, Y. Lee, B. S. Bae and T. S. Kim, *Adv. Eng. Mater.*, 2021, **23**, 2001280.
 28. N. Akamatsu, W. Tashiro, K. Saito, J.-i. Mamiya, M. Kinoshita, T. Ikeda, J. Takeya, S. Fujikawa, A. Priimagi and A. Shishido, *Sci. Rep.*, 2014, **4**, 5377.
 29. R. Taguchi, N. Akamatsu, K. Kuwahara, K. Tokumitsu, Y. Kobayashi, M. Kishino, K. Yaegashi, J. Takeya and A. Shishido, *Adv. Mater. Interfaces*, 2021, **8**, 2001662.
 30. R. Taguchi, A. Fujisawa, M. Kishino, K. Kuwahara, N. Akamatsu, M. Fukuhara and A. Shishido, *AIP Adv.*, 2022, **12**, 015324.
 31. I. Donelli, G. Freddi, V. A. Nierstrasz and P. Taddei, *Polym. Degrad. Stabil.*, 2010, **95**, 1542–1550.
 32. M. Kishino, K. Hisano, Y. Kishimoto, R. Taguchi and A. Shishido, *J. Phys. Chem. C*, 2023, **127**, 14510–14517.
 33. M. Kishino, K. Matsumoto, Y. Kobayashi, R. Taguchi, N. Akamatsu and A. Shishido, *Int. J. Fatigue*, 2023, **166**, 107230.
 34. K. Noda, A. Takahara and T. Kajiyama, *Polymer*, 2001, **42**, 5803–5811.
 35. A. Takahara, K. Yamada, T. Kajiyama and M. Takayanagi, *J. Appl. Polym. Sci.*, 1981, **26**, 1085–1104.
 36. M. Psczcola, M. Jaczewski and C. Szydowski, *Appl. Sci.*, 2019, **9**, 846.
 37. O. L. Cruz-González, A. Ramírez-Torres, R. Rodríguez-Ramos, J. A. Otero, R. Penta and F. Lebon, *Appl. Eng. Sci.*, 2021, **6**, 100037.
 38. J. Lai and A. Bakker, *Polym. Eng. Sci.*, 1995, **35**, 1339–1347.
 39. J. Lai and A. Bakker, *Scripta. Metall. Mater.*, 1993, **28**, 1447–1452.
 40. E. Ito and Y. Kobayashi, *J. Appl. Polym. Sci.*, 1980, **25**, 2145–2157.
 41. I. H. Sahputra and A. T. Echtermeyer, *Macromol. Theor. Simul.*, 2015, **24**, 65–73.
 42. Z. Bartczak, *Macromolecules*, 2005, **38**, 7702–7713.